

Finite element simulation of the structural integrity of endothelial cell monolayers: a step for tumor cell extravasation

A. Nieto, J. Escribano, F. Spill, J.M. Garcia-Aznar, M.J. Gomez-Benito

Highlights

- Aim: Understand how the adhesions between cells that form the endothelial monolayer are broken to allow cells to extravasate.
- We model the dynamics of cell-cell junctions rupture produced in the endothelial monolayer by the effect of Calcium waves.
- Endothelial cells are simulated as linear elastic materials
- Cell-cell adhesions of the monolayer are simulated by means of a catch bond law.
- We study the effect of the blood vessel diameter on the rupture of the adhesions of monolayer.

Finite element simulation of the structural integrity of endothelial cell monolayers: a step for tumor cell extravasation

A. Nieto^a, J. Escribano^a, F. Spill^b, J.M. Garcia-Aznar^a, M.J. Gomez-Benito^a

^a*Multiscale in Mechanical and Biological Engineering (M2BE), Department of Mechanical Engineering, Aragón Institute of Engineering Research (I3A), University of Zaragoza, Zaragoza, Spain*

^b*School of Mathematics, University of Birmingham, Birmingham, B15 2TT, UK*

Abstract

Cell extravasation is a crucial step of the metastatic cascade. In this process, the circulating tumor cells inside the blood vessels adhere to the cell monolayer of the blood vessel wall and passes through it, which allows them to invade different organs and complete metastasis. In this process, it is relevant to understand how the adhesions between cells that form the endothelial monolayer are broken, resulting in intra-cellular gaps through which tumor cells are able to extravasate the blood vessel wall.

Within this process, we focus on studying the dynamics of cell-cell junctions rupture produced in the endothelial monolayer by the effect of Calcium waves. The regulation of this monolayer is of vital importance, not only in metastasis, but also in diseases such as pulmonary edema or atherosclerosis.

In order to understand this rupture dynamics in greater depth, we propose a hybrid model that simulates endothelial cells as an elastic material and cell-cell adhesions of the monolayer by means of a catch bond law.

We study the effects that the cell contraction caused by a Calcium wave presents on the endothelial monolayer depending on the diameter of the blood vessel. For this purpose, we develop a three-dimensional model to study the effect of the different blood vessel diameters.

The results indicate that there are greater tractions on the joints located in vertices common to several cells. This led to the formation of openings in the endothelial monolayer, through which extravasation of tumor cells could occur. For the different geometries studied, no significant effect of the blood

vessel diameter on the rupture of the adhesions of monolayer is observed.

Keywords: Cell extravasation, endothelial monolayer, adhesion rupture, finite element

1 Acronyms

AJs	—	Adherens Junctions.
VE-Cadherin	—	Vascular endothelial cadherin.
HUVECs	—	Human umbilical vein endothelial cell.
ECM	—	Extracellular Matrix.
FAJs	—	Focal Adherens Junctions.
FAs	—	Focal Adhesions.
LAJs	—	Linear Adherent Junctions.
RSFs	—	Radial Stress Fibers.

3 1. Introduction

4 Cell extravasation of cancer cells is part of the metastatic cascade. In
5 this process, cancerous cells depart from the primary tumor and are able to
6 intravasate into the blood flow. Once inside, these cells move through the
7 blood until they arrest in the blood vessel wall, which consists of a monolayer
8 of endothelial cells (i.e. the endothelium), and extravasate in order to colo-
9 nize a new tissue or organ. This is possible due to the creation of gaps in the
10 cellular monolayer of the blood vessel. The endothelium is formed of a thin
11 lamina of endothelial cells that are separated from the outer ones by an elas-
12 tic membrane. The endothelial cells are joined by protein complexes such as
13 vascular endothelial cadherin (VE-Cadherin), Nectin, PECAM, etc [1], that
14 form a dynamic structure in which adhesions are broken and rebuilt all the
15 time. This dynamic is responsible for the creation of the openings through
16 which the cancer cells can extravasate [2]. Cell transmigration involves the
17 generation of mechanical forces through the actomyosin cytoskeleton and the
18 deformation of the endothelium whose mechanical properties provide passive
19 resistance [3]. Different studies have revealed that endothelial monolayer
20 properties are crucial in gap formation [4] and that higher levels of junc-
21 tion stiffness can reduce paracellular extravasation [5]. This suggests the
22 importance of analyzing the main drivers behind cell-cell adhesion.

23 The formation and maintenance of tissues are not only driven by chemical
24 but also mechanical processes. The endothelium is subjected to a dynam-
25 ically changing mechanical environment (i.e. oscillations in blood flow-rate
26 and pressure conditions) which can induce strains in the lining of arteries.
27 Moreover, tangential cyclic forces maintained in time can also change the me-
28 chanical properties of the tissue itself [4]. The endothelium additionally acts
29 as a barrier. It must allow immune system cells to go through while blocking
30 pathogens, blood or tumor cells. One of the key points in this mechanism is
31 the contraction of the actomyosin cytoskeleton of endothelial cells, although
32 there are many points open to be investigated.

33 Despite the clinical relevance of metastasis and tumoral extravasation,
34 little is known about the mechanical environment that regulates it [6]. The
35 idea that cellular contraction can impact the barrier function of the endothe-
36 lial monolayer was pointed out in the 70s when several proteins involved in
37 this process were identified [7]. In the last four decades, it has been proven
38 that this mechanical contraction is key in both the mechanical behavior and
39 the development of cells and tissues [8]. In order to improve the understand-
40 ing of this process, two main modeling approaches are adopted: *in vitro*
41 and *in silico* models. *In vitro* models reproduce the simplified conditions of
42 cell extravasation by controlling the main elements involved (i.e. cells, ex-
43 tracellular matrix (ECM), growth factors). Although the microenvironment
44 cannot be perfectly controlled in these models, they allow comparative anal-
45 ysis and the study of cell-cell and cell-extracellular matrix interactions [9].
46 Within these *in vitro* models, microfluidic devices allow greater control of
47 the microenvironmental variables. They have been used both for the study
48 of cell migration and the intravasation of mechanical barriers [10] and cell
49 extravasation [11]. Funamoto et al. [12] studied the behavior of endothelial
50 monolayers under hypoxic conditions using microfluidic channels and Valent
51 et al. [13] measured contraction forces of human umbilical cord endothelial
52 cells (HUVECs) using traction force microscopy. Few numerical models have
53 focused on the simulation of cell extravasation *in silico*. Chen et al. [14] simu-
54 lated cancer cell deformation during intra- and extravasation, they considered
55 both chemotactic and durotactic factors. Ramis-Conde et al. [15] created a
56 mathematical model focused on intravasation of tumoral cells with a multi-
57 scale focus taking into account both intra- and inter-cellular proteins and the
58 shape of the blood vessel. Regarding cellular monolayer, González-Valverde
59 and García-Aznar [16] created a hybrid model focused on the simulation of
60 the dynamic of cellular monolayer combining numerical discrete and continu-

61 ous models. Recently, Escribano et al. [2] created a discrete two dimensional
62 (2D) model in which they analyzed the dynamic behavior of an endothelial
63 monolayer. They studied how different mechanical factors influence cell-cell
64 adhesion rupture and the consequent generation of gaps in the monolayer.

65 To regulate barrier function, permeability factors influence the following
66 elements of the cellular structure: cell-cell adhesion complexes, cytoskele-
67 ton and integrin-ECM adhesions. First, cell-cell adhesion complexes are the
68 last line of defence against vascular permeability. VE-Cadherins are chemi-
69 cally modified through phosphorylation, thus impacting the stability of en-
70 dothelial junctions [17]. Phosphorylation regulates the interplay between the
71 VE-Cadherin complex and other complexes, which at last determine the me-
72 chanical strength of cell-cell adhesions. Second, the myosin motor activity
73 in the cytoskeleton is key when permeabilization occurs [18], stabilizing cell
74 structure when it is close to actin bundles and networks [19]; whereas, when
75 actin is mainly found on radial stress fibers (RSFs), instability and traction
76 forces increase in the cytoskeleton [20]. Changes in actin bundles seem to
77 influence the local structure and cell-cell adhesion forces. Changes in actin
78 bundles tend to increase distance between cell-cell adhesions, while radial
79 actin bundles arise from those connected to cell-cell complexes. Thus, spa-
80 tial distribution of traction forces in actomyosin structures seems to be key
81 in permeability of endothelial cells [4].

82 VE-cadherins do not transmit force linearly in cell-cell adhesions. It is
83 a two-phase process. First, in the absence of contraction forces, the pre-
84 dominant adhesions in a monolayer are linear adherens junctions (LAJs).
85 The formation of RSFs in endothelial cells causes movement of the actin
86 cytoskeleton into the cell, which reduces the presence of actin bundles that
87 serve as connecting elements for LAJs. This reduction of actin destabilizes
88 the LAJs and, therefore, for the creation of gap openings in the endothelial
89 wall. Second, this destabilization, caused by contraction forces in the cells,
90 has another opposite effect: the areas with the presence of VE-cadherin ad-
91 hesions resist, resulting in the appearance of focal adherens junctions (FAJs).
92 It is thought that this process of formation of the FAJs could be a stochas-
93 tic process or could be induced by unknown inhomogeneities of the LAJs at
94 submicroscopic levels [4]. When these adhesions begin to withstand traction
95 forces, the α -catenin begins to lengthen and vinculin recruitment occurs in
96 the adhesions. Once these bonds have been strengthened, a signaling takes
97 place leading to the restoration of the LAJs. This behavior causes a very
98 active and changing dynamics in the monolayer.

99 The structure of endothelial cells is determined by the dynamic interac-
 100 tion between cell-ECM adhesions, cytoskeletal networks and cell-cell adhe-
 101 sions whose integrity determines barrier function [4]. Cell-cell adhesions are
 102 formed by a large number of proteins. Among these proteins, VE-Cadherin
 103 stands out as a key player in force transmission. Several studies [21, 22]
 104 have concluded that loss of VE-Cadherin adhesions affects other cell-cell ad-
 105 hesions, deteriorates the integrity of the barrier function and leads to deep
 106 changes in the cytoskeletal structure. The VE-Cadherin complex is connected
 107 to the actin cytoskeleton through α -catenin forming AJs (endothelial adher-
 108 ent junctions) which play a key role in barrier function. Actin bundles close
 109 and parallel to cell-cell adhesions improve the integrity of these adhesions,
 110 while RSFs in the center of the endothelial cell are associated with lower
 111 stability [23]. Cell-ECM adhesions control the organization and contractility
 112 of the actomyosin network. These integrin-based adhesions are organized in
 113 FAs (focal adhesions) and constitute signalling centers that sense chemical
 114 and mechanical information. Thus, there is a mechanical feedback between
 115 the actomyosin cytoskeleton and the ECM through FAs which matches the
 116 mechanical environment from cellular to structural level [24].

117 The aim of this work is to simulate the endothelial monolayer and cell-
 118 cell adhesions through a new constitutive model. This model will take into
 119 account the dynamic behavior of cell adhesions and its stochastic nature. The
 120 model will investigate the influence of blood vessel diameter in the formation
 121 of opening gaps in the cellular monolayer through which tumor cells could
 122 extravasate. Unlike previous works [2] the model will consider the three
 123 dimensional (3D) geometry of the vessels and cells, which will be simulated
 124 as continuum elements.

125 2. Materials and Methods

In this work, we simulate the endothelial cell monolayer as a continuum
 medium, where the balance of linear momentum is satisfied in all the mono-
 layer:

$$\nabla \cdot \sigma + \mathbf{f} = \mathbf{0} \quad (1)$$

126 With σ the Cauchy stress tensor and \mathbf{f} the body force per unit of current
 127 volume and $\nabla \cdot$ the divergence operator.

128 This equation is solved by means of the Finite Element approach, where
 129 we discretized the monolayer domain, distinguishing between the cell body
 130

131 and the cell-cell adhesions. Actually, the cell body is discretised by solid
 132 elements, and the cell-cell adhesions are discretized by truss elements that
 133 connect nodes from different cell discretizations.

134 Therefore, in the following subsection, we present the basics of how cell-
 135 cell interactions are simulated. Next, we introduce the mathematical model
 136 used to describe the cell mechanical behaviour. Finally, we show how these
 137 mathematical models have been numerically implemented in a FE-based ap-
 138 proach.

139 *Modeling and simulations of cell-cell adhesion*

140 Previous works explain cell-cell adhesion through discrete [25], continuous
 141 [26] and hybrid [16] models, they include the effect of cell-cell interactions
 142 as interaction forces or potentials, but in general they not consider explicitly
 143 adhesions as a different element.

144 Experimental evidences show that cadherins bonds increase their lifetime
 145 if subjected to mechanical forces [27, 28, 29, 30]. Moreover, the catch bond
 146 law are widely use in literature to explain cell adhesions in general [27] and
 147 it is a widely accepted model in the modelling literature [2, 30, 29]. Thus,
 148 the failure of the cell-cell joints is defined as a *catch-slip bond* law [31] that
 149 provides a stochastic behavior to the rupture of these adhesions. This law
 150 adapts to the mechanical behavior observed in VE-cadherins, where the joints
 151 subjected to low forces are unstable. As the stress in the joints increases, they
 152 become more stable until a point where the joints are not able to withstand
 153 the force and the probability of rupture begins to grow exponentially. Thus,
 154 we assume the probability of rupture or binding follows this law:

$$k_{ub}(F) = e^{\varphi_c - \frac{F}{F_{sat}}} + e^{\frac{F}{F_{sat}} - \varphi_s} \quad (2)$$

$$prob_{ub} = 1 - e^{-k_{ub}\Delta t} \quad (3)$$

155 where k_{ub} is the ratio of failure which is a function of the ratio between the
 156 force F in the cell-cell adhesion and F_{sat} parameter of the union saturation
 157 force and φ_c and φ_s are adimensional force parameters for the curve of *catch*
 158 and *slip bond*, respectively. It is assumed that the effect of compressive forces
 159 is not able to cause damage to the joints. The probability of rupture, $prob_{ub}$,
 160 behaves as an exponential function that depends on the force that the union
 161 supports ($k_{ub}(F)$) and the time that the union is supporting this force (Δt),
 162 since in biological processes of rupture, the time that a force acts on a material

163 is crucial in the effect that force has on the material (e.g. pressure ulcers in
 164 the skin). We assume the time increment is small enough to consider the
 165 force constant during this time interval.

166 Unbinding is represented by the loss of rigidity of the adhesion by a
 167 variable of damage (d). To compute if the adhesion is bound or unbound, we
 168 generate a random number (τ) from a uniform distribution between 0 and 1,
 169 which is compared with the probability of unbinding:

$$d = \begin{cases} 0.00 & \tau < prob_{ub} \\ 0.99 & \tau \geq prob_{ub} \end{cases} \quad (4)$$

170 The evolution of this law (figure 1) follows the behavior of VE-cadherins
 171 observed in experiments [27, 28, 29, 30]. When the traction forces are low,
 172 there is a high vinculin recruitment by the VE-cadherins, so the FAJs have
 173 a lower rigidity, which is reflected in the higher probability of rupture in the
 174 area of the graph with negative slope. After this phase, when the traction
 175 forces increase and are within a range in the valley of the curve, the joints
 176 work in their optimum zone, so they present a low rupture probability. As
 177 the traction forces continue to rise, the probability of rupture increases again
 178 exponentially. In fact, for the same force, there can be a big difference in
 179 the probability of unbinding depending on whether this force is applied in a
 180 large ($\Delta t = 0.01$ s) or small ($\Delta t = 0.00001$ s) time increment.

181 In a similar way as the law of unbinding, the formation of cell-cell ad-
 182 hesions is also characterized by a stochastic probability of binding ($prob_b$),
 183 which depends on the separation between cells:

$$k_b(L_{cadh}) = D_{cadh} \left(1 - \frac{L_{cadh}}{L_{lim}} \right) \quad (5)$$

$$prob_b = 1 - e^{-k_b \Delta t} \quad (6)$$

184 where k_b is the binding ratio, D_{cadh} represents the density of VE cadherins
 185 available for binding in the monolayer, L_{cadh} is the current length of the
 186 adhesion, L_{lim} is the maximum length for which the union is allowed and,
 187 Δt is the time increment.

188 Binding is represented by the restoration of initial rigidity of the adhesion.
 189 To compute if the adhesion is bound or not we again generate a random
 190 number (τ) from a uniform distribution between 0 and 1, which is compared
 191 with the probability of binding:

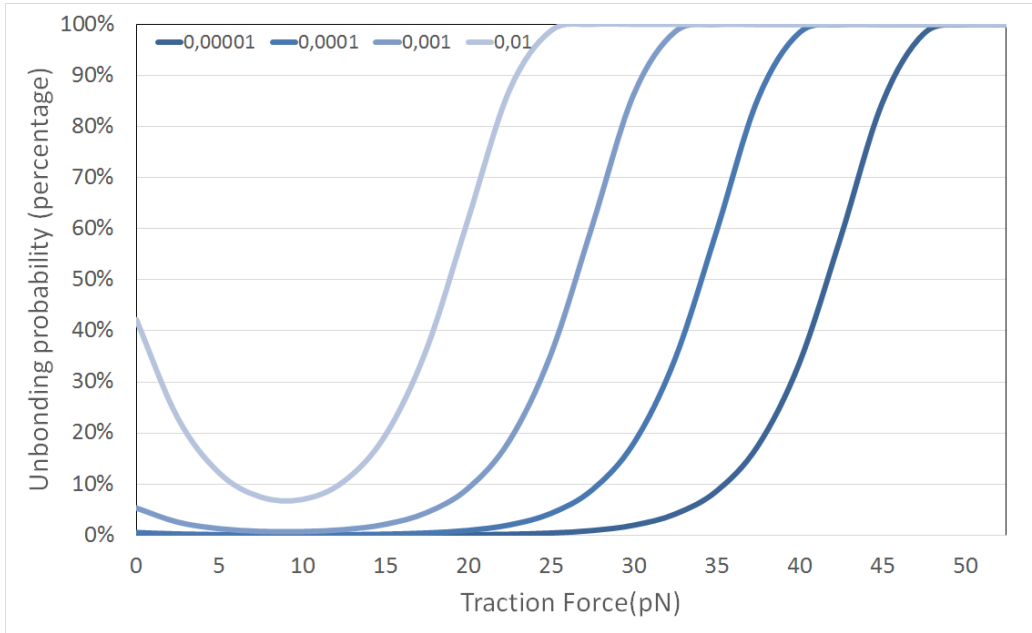


Figure 1: Evolution of the probability of unbinding of cell-cell adhesions as a function of the traction forces they support and their duration (Δt in seconds).

$$d = \begin{cases} 0.99 & \tau < prob_b \\ 0.00 & \tau \geq prob_b \end{cases} \quad (7)$$

192 The evolution of the formation of cell-cell adhesions is observed in figure
 193 2. Once the maximum cadherin length has been exceeded, the probability
 194 that the adhesion occurs is null. The density of VE-cadherin available for
 195 union (D_{cadh}) modifies the slope of the function, so it establishes a maximum
 196 union probability of 45%.

197 When the adhesion is unbound we assume that the mechanical properties
 198 of the cadherin is reduced to 1% of its original value due to its damage. In
 199 contrast when it binds again, adhesion recovers its initial mechanical prop-
 200 erties.

201 *Modeling cell mechanics*

202 We consider cells behave as an hyperelastic Neo-hookean material. Thus,
 203 the strain energy function reads:

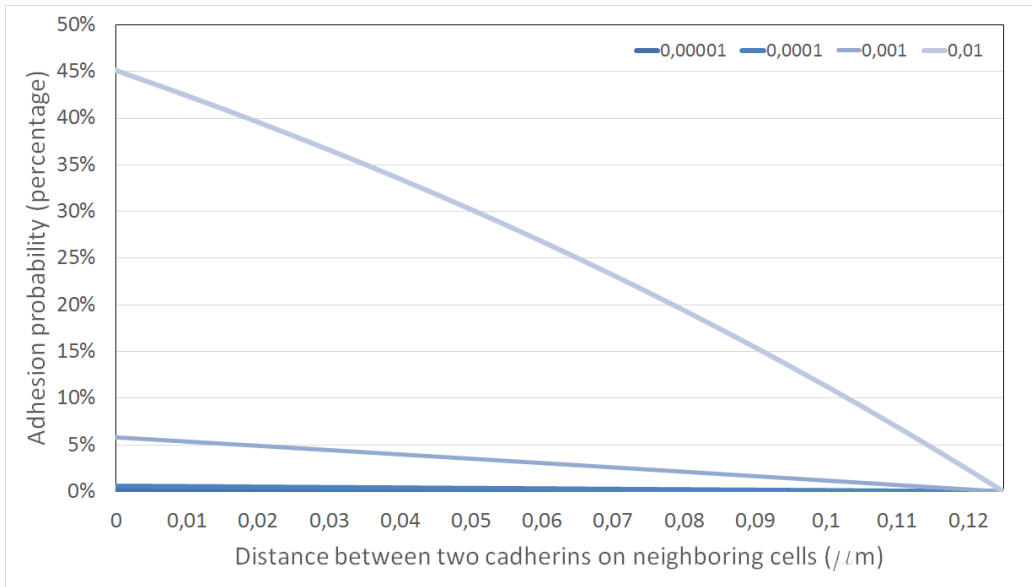


Figure 2: Evolution of the probability of cell-cell adhesions as a function of the distance between two cadherins on neighboring cells and the increase in time (seconds). $D_{cadh} = 60$.

$$U = C_{10}(\bar{I}_1 - 3) + \frac{1}{D_1}(J - 1)^2 \quad (8)$$

204 Where \bar{I}_1 is the first invariant of the right Cauchy-Green deformation tensor,
 205 J is the elastic volume ratio and C_{10} and D_1 are material parameters. For
 206 endothelial cells, material parameters are set to 173Pa and $6 \cdot 10^{-4} Pa^{-1}$
 207 respectively which are equivalent to an initial elastic modulus of 1000Pa
 208 and a Poisson ratio of 0.45 based on experimental data from previous works
 209 [32, 33, 34].

210 We assume finite deformations due to the large strains that VE-cadherin
 211 suffers during gap formation.

212 In the case of blood vessels of infinite radius compared to the endothelial
 213 cell, we will adopt a plane stress assumption. Nevertheless, for the blood
 214 vessel of known diameter a 3D model is adopted (figure 6).

215 The endothelial monolayer is a very dynamic structure exposed to very
 216 variable boundary conditions. Thus, certain simplifying hypotheses have to
 217 be established in order to carry out its modeling. The endothelial cells are
 218 immersed in an ECM, which acts as a substrate that holds them in place
 219 when mechanical conditions are not severe, and they are also exposed to the

220 internal pressure exerted by blood flow which in this first model is neglected.
 221 Henceforth, the radial displacement experienced by the monolayer can be
 222 assumed to be relatively small and have little influence on the rupture of
 223 cell-cell adhesions. We assume endothelial cells are perfectly anchored to the
 224 vessel wall through the basal membrane which allow displacements in the
 225 circumferential and longitudinal direction and avoid radial displacements.
 226 Therefore, we neglect the deformation of the blood vessel diameter. Hence,
 227 in the 3D endothelial monolayer model displacements in the radial direction
 228 are set to zero. In addition, at the free ends of the monolayer, displacements
 229 are constrained in all directions, we assume the blood vessel is long enough,
 230 thus this boundary condition do not affect model results.

231 The cell monolayer is continuously subjected to normal and tangential
 232 stresses caused by the blood flow circulating within it. However, these
 233 stresses are not directly causing changes in endothelial permeability. One of
 234 the most significant permeability mechanisms of the endothelial monolayer is
 235 through increased intracellular Calcium concentration (Ca^{2+}). The increase
 236 in Calcium concentration activates signaling pathways that affect both the
 237 structural organization of the cytoskeleton and the cell-cadherin-VE adhe-
 238 sions [35]. This is because Calcium-dependent proteins cause the endothelial
 239 cells to contract, leading to increased traction forces supported by adhesions.
 240 The propagation of Calcium through waves has been widely accepted as a
 241 factor which changes the architecture of the endothelial monolayer [36].

242 The loading conditions simulated in the model are these Calcium waves
 243 in order to observe the effect they have on the rupture and remodelling
 244 of the VE-cadherins and, therefore, on the permeability of the endothelial
 245 monolayer. The wave begins at one end of the endothelial cell monolayer
 246 and advances in the longitudinal direction of the geometry. The distribution
 247 of the contraction is shown in figure 3 where each line represents a different
 248 column of cells, its amplitude is estimated between 1% and 3% [37].

249 To simulate cell contraction due to calcium wave propagation, we assume
 250 this calcium wave produces volumetric cell contraction or expansion. At any
 251 time we consider three configurations, the undeformed configuration (Ω_0),
 252 the deformed configuration (Ω_t) and an intermediate configuration of con-
 253 traction (or expansion) due to the calcium wave (Ω_{Ca+}) which in general is
 254 not compatible [38, 39].

255 The total deformation gradients maps any point in the undeformed (ma-
 256 terial) configuration (\mathbf{X}) to a point in the deformed (spatial) configuration
 257 (\mathbf{x}):

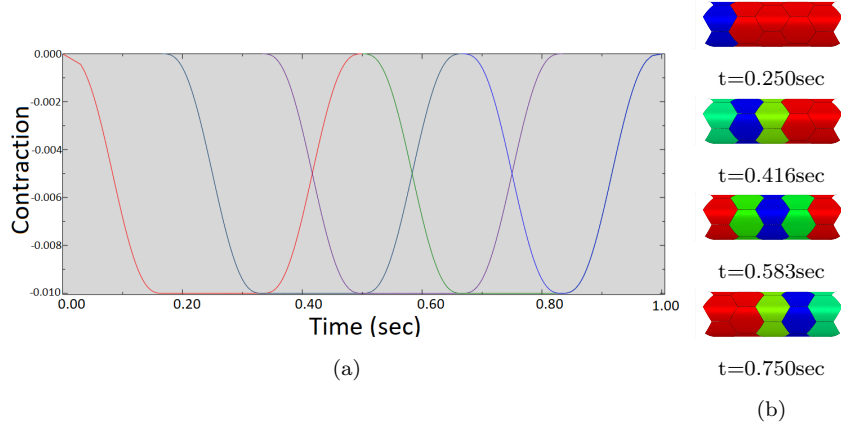


Figure 3: Evolution of the contraction due to calcium wave for each column of cells as a function of time, red lines correspond to the first cell column, dark blue for the second column, purple to the third cell column, green for the fourth and so on (a), and spatial evolution of this contraction at different timepoints in the blood vessel, red means minimum contraction and blue maximum, green means intermediate value of contraction (b).

$$\mathbf{F} = \frac{\partial \mathbf{x}}{\partial \mathbf{X}} \quad (9)$$

258

259 We make use of the multiplicative decomposition [40] of the total defor-
 260 mation gradient \mathbf{F} :

$$\mathbf{F} = \mathbf{F}_e \cdot \mathbf{F}_{Ca+} \quad (10)$$

261 where \mathbf{F}_e is the isothermal deformation gradient and \mathbf{F}_{Ca+} is the deformation
 262 gradient produced by the volume change due to the calcium wave:

$$\mathbf{F}_{Ca+} = -a_i(t)\alpha c_{Ca+} \mathbf{1} \quad (11)$$

263 where c_{Ca+} is the calcium concentration, α is a constant, $\mathbf{1}$ is the second
 264 order unit tensor and $a_i(t)$ is evolution in time of the amplitude of the calcium
 265 wave for each cell column (i).

266 Note that these equations are mathematically similar to equations de-
 267 scribing thermoelastic systems, to see the full formulation refer to [40].

268 This calcium wave produces contraction in the endothelial monolayer and
 269 it is assumed to be moving through the different cell columns with time. As

270 a first approach, the amplitude of the calcium wave in each cell column (i)
 271 is assumed to depend just on time (t). The calcium wave enters smoothly in
 272 the cell column, it remains for a sixth of a second and it also leaves the cell
 273 column smoothly. Thus, the amplitude ($a_i(t)$) of the calcium wave in each
 274 cell column is described through:

$$a_i(t) = \begin{cases} 0.0 & 0 \leq t \leq t_i \\ \xi^3(10 - 15\xi + 6\xi^2) & t_i \leq t \leq t_{i+1} \\ 1 & t_{i+1} \leq t \leq t_{i+2} \\ 1 - \xi^3(10 - 15\xi + 6\xi^2) & t_{i+2} \leq t \leq t_{i+3} \\ 0 & t_{i+3} \leq t \end{cases} \quad (12)$$

275 where $t = \frac{t-t_i}{t_{i+1}-t_i}$ and $t_i = \frac{1}{6}i$.

276 Due to the small dimensions of the adhesions with respect to the cell size,
 277 volume change of the adhesions due to calcium wave is neglected.

278 In summary, the model simulates the binding and unbinding of cell-cell
 279 adhesions depending on the mechanical environment they are subjected to,
 280 their deformation (length of the adhesion with respect to the maximum) and
 281 traction forces transmitted through the adhesion. The only load considered is
 282 the calcium wave which contracts the cells and deforms the adhesions (Figure
 283 4).

284 *Numerical Implementation*

285 To carry out the simulations, we use the commercial FE software ABAQUS.
 286 We develop a material user subroutine (UMAT) to define the mechanical
 287 behavior of the truss elements that simulate cell-cell adhesion and several
 288 Python scripts to create the geometry of the model. We assume cells are
 289 arranged in the monolayer as regular hexagons following previous works
 290 [2, 41, 42, 43]. In fact, to generate the geometry we fix four main parameters:
 291 the characteristic length of the endothelial cells (in μm), which corresponds
 292 to the length of the side of the hexagonal cell, the number of VE-cadherins
 293 in each side of the cell and the number of endothelial cells that form the en-
 294 dothelial monolayer and the diameter of the vessel. To discretize the model,
 295 in the case of the cells, we use linear shell element (S3, S4) for the 3D vessels
 296 and plane stress quadrilateral or triangular linear elements (CPS3, CPS4)
 297 in the vessels of very large radius; whereas for the adhesions we use linear
 298 truss elements (T3D2 in 3D and T2D2 in 2D).

299 Next, we present all the step that we use to define the FE model to
 300 simulate endothelial cell monolayers:

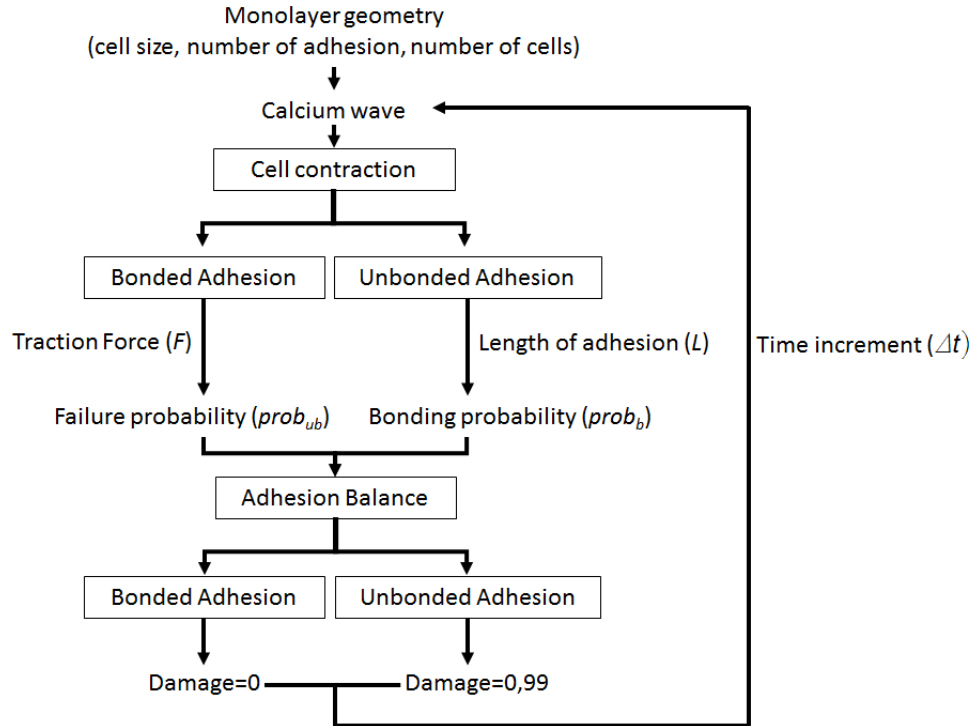


Figure 4: Scheme of the model, once we fix the geometry of the monolayer the calcium wave contracts the cells modifying the mechanical state of the cells and the adhesions. When an adhesion is bonded it can unbind depending on the force in the adhesion and the time increment; when an adhesion is unbonded it can rebond if it reduces its length. After balance of adhesions, mechanical properties of adhesions are updated and a new time increment starts.

- 301 1. We generate a cell. All the cells of the monolayer will be generated
302 from this first one, we assume homogeneity of geometry and structure
303 between cells. We start by generating the hexagonal cell with side equal
304 to the value provided by the user (figure 5). We estimate a thickness
305 of 500 nm for the endothelial monolayer [44, 45], however there is high
306 variability for the thickness in literature [46].
- 307 2. To create cell-cell adhesion, we partition cells sides, the algorithm cre-
308 ated will iterate n times making a number of partitions such that the
309 number of adhesions per side is $2^n + 1$ (figure 5, with $n = 3$).
- 310 3. With the cell already defined, the structure of the endothelial mono-
311 layer is formed. Cells are positioned at a fixed distance defined by the

312 user, which corresponds to the length of the VE-cadherins (50 nm for
 313 our simulation [47]). The cells are transferred symmetrically in such
 314 a way to obtain the distribution described by the user based on the
 315 number of cells in each column.
 316 4. After obtaining the geometric distribution of the cells in the unde-
 317 formed configuration, we run a *script* which can determine the position
 318 of FAJs in the monolayer. First, we identify all points of interest likely
 319 to form a cell-cell adhesion. Second, this list of points is compared
 320 to the relative distance between subsets of two points to know if they
 321 form an adhesion. We verify whether the subset of points is at a dis-
 322 tance equal to the length of the VE-cadherins. If it is and the points
 323 belong to two different cells, a cell-cell adhesion is created. The initial
 324 model is two dimensional and a change to cylindrical coordinate system
 325 transforms it into a three dimensional monolayer.

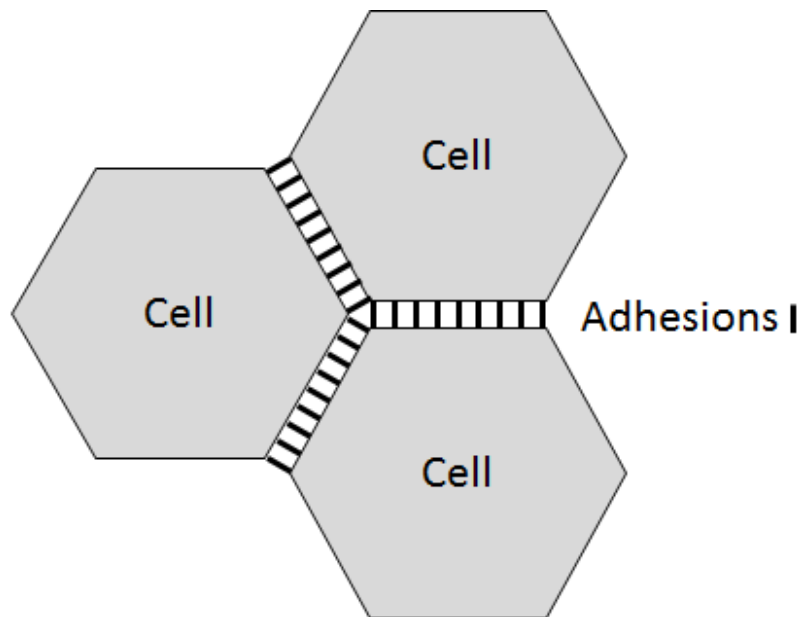


Figure 5: Scheme of cell geometry generation and cadherins attachment points

326 We assume VE-cadherins support just axially load and they follow the
 327 catch bond and rupture law previously described. Therefore, FAJs work only
 328 axial, so working with elements that also withstand bending stresses (e.g.
 329 *beams*) would not adequately simulate their behavior; if the cells joined by an

330 adhesion suffer opposite parallel displacements (shear stresses), the elements
331 would be acting as LAJs (tangential stresses) since their arrangement would
332 be nearly parallel to the membrane.

333 Due to the dynamic behavior of VE-cadherins, these may suffer many
334 changes, binding and unbinding, during the simulation. When the adhesion
335 is defined as unbound its elastic modulus is reduced to 1% of the original
336 value, thus there will be a loss of stiffness in the joint. These losses of stiffness
337 cause a great non-linearity in the stresses suffered by the adhesions making
338 it difficult to converge in a static analysis, since FE program will continue to
339 iterate until these discontinuities are small enough and the tolerances of the
340 equilibrium are satisfied.

341 Thus, non-linear static analyzes can be unstable. In our case, changes
342 in material stiffness can lead to local instabilities where there is a transfer
343 of strain energy from one part of the model to another, causing the global
344 methods used to arrive at the solution that does not work. This is solved
345 by automatic stabilization with a constant damping coefficient, in case a re-
346 gion becomes unstable, it absorbs part of the deformation energy dissipating
347 it through the damping. In fact, the numerical solution of cancer related
348 simulations is complex [48, 49].

349 All the simulations were executed on a High-Throughput Computing
350 (HTC) environment which can reduce the required times to run those simula-
351 tions by parallelizing them. The averaged execution time of each simulation
352 was 5 hours using 1 CPU and 1024 MB of RAM.

353 The VE cadherins suffer large deformations, so evaluating the deforma-
354 tions and stresses with respect to their undeformed configuration would not
355 provide real solutions. Therefore, the simulation is performed with the hy-
356 pothesis of finite strains. The model parameters used in the simulation are
357 summarized in Table 1.

358 Diameters of blood vessels are highly variable. In the bat's wing these
359 diameters range from $76.2\mu\text{m}$ and $52.6\mu\text{m}$ in the veins and arteries respec-
360 tively to $3.7\mu\text{m}$ in a capillary [50]. However, in humans the diameter of blood
361 vessels ranges from around $8\mu\text{m}$ in capillaries to more than 1cm in large ar-
362 teries [51, 52]. In this work, we study three different blood vessel diameters
363 $11.1\mu\text{m}$, $13.86\mu\text{m}$, $16.64\mu\text{m}$ and an infinite diameter of the blood vessel com-
364 pare to the cell diameter ($10\mu\text{m}$) (figure 6). To determine if the blood vessel
365 diameter has an influence in the formation of openings in the blood vessels.

366 In simulations, we use models with a maximum of 33 adhesions per cell
367 side which show a good compromise between accuracy and computational

φ_c	2.5
φ_s	0.2
F_{sat}	$3.3pN$
L_{lim}	$0.125\mu m$
D_{cadh}	60

Table 1: Model parameters used in the simulation.

368 cost. If we increase the number of cadherins per cell side, results would be
369 more realistic; however, it would considerably increase the computation time
370 to calculate the cell-cell adhesions.

371 We simulate the mechanical behavior of the endothelial monolayer and
372 the damage suffered by the cell-cell adhesions caused by a Calcium wave that
373 travels through the monolayer. The intensity of the cellular contraction has
374 been varied for three different cases ($\alpha c_{Ca+} = 0.01, 0.02, 0.03$).

375 3. Results and Discussion

376 First, we analyse the location of the stress concentrations in the endothe-
377 lial cells. The maximum stresses are generally found in the vertices where
378 three different cells meet (Figure 7).

379 These results indicate that a higher stress in the joints located at these
380 points made them more prone to break as they withstand higher stresses
381 than others (Figure 7). This implies that the openings in the endothelial
382 monolayer are normally formed in the adhesions located in these vertices,
383 suggesting that extravasation is more likely to occur in these areas.

384 We clearly observe different failure patterns of the endothelial monolayer.
385 The endothelial monolayer is a very active and changing dynamic structure.
386 This causes its mechanical behavior to be very different for different me-
387 chanical environments. Three main phases of work can be distinguished for
388 VE-cadherins: the resting phase, the working phase and the rupture phase.
389 The resting phase is unstable, this situation occurs when the contraction
390 forces in a monolayer are very low, that is, the Calcium wave circulating in
391 the monolayer does not cause a high contraction, so the stresses experienced
392 by VE-cadherins are very low (Figure 8). When the traction forces are very
393 low there is no vinculin binding recruitment [53], thus the unions are not very
394 stable and their rigidity is low. This situation is reflected in the model, the
395 monolayer presents a high damage in the VE-cadherins. However, since there

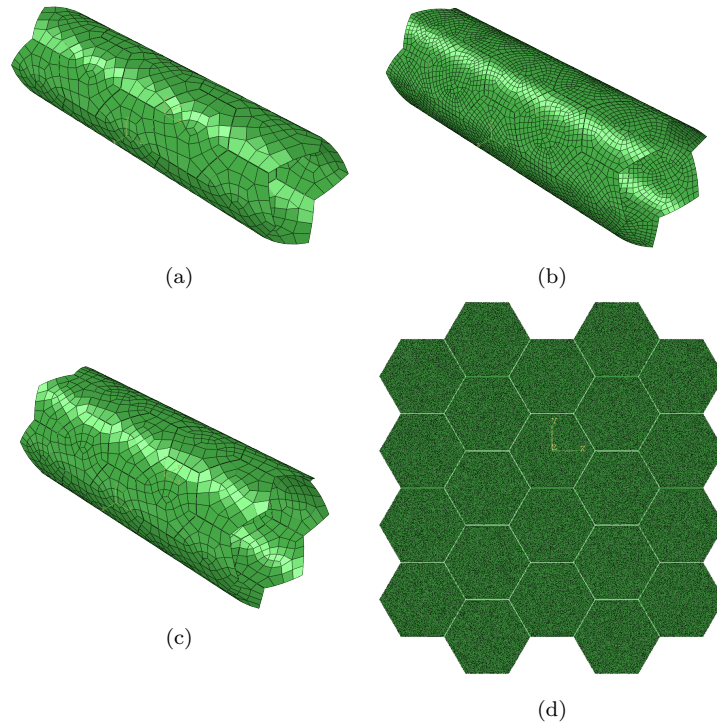


Figure 6: Three-dimensional models studied: (a) small diameter ($10.1\mu\text{m}$), (b) medium diameter ($13.86\mu\text{m}$), (c) large diameter ($16.64\mu\text{m}$) and (d) very large diameter (∞)

396 is very little deformation of the adhesions, the possibility of their recovery is
 397 high (equation 6), which creates a very active dynamic behaviour in which
 398 the unions unbind and bind constantly. This phase would correspond to the
 399 first part of the figure 1 where the probability of rupture is high just before
 400 reaching the “valley” where this probability decreases.

401 When the forces exceed the failure limit of cell-cell adhesions, they begin
 402 to break. The more adhesions are broken, the more stresses must withstand
 403 the remaining adhesion so their probability of unbinding increases. This
 404 made the openings in the monolayer to be similar in shape to the propagation
 405 of a crack (figure 9). This does not occur in normal working conditions of
 406 the endothelial monolayer, but it could happen in extreme cases in which
 407 the integrity of the monolayer is compromised. For the three-dimensional
 408 studied cases, the greater the severity of the failure, the greater the radius
 409 of the endothelial monolayer (figure 10). In larger monolayers there is a
 410 greater effect of the contraction on the forces suffered by the adhesions as

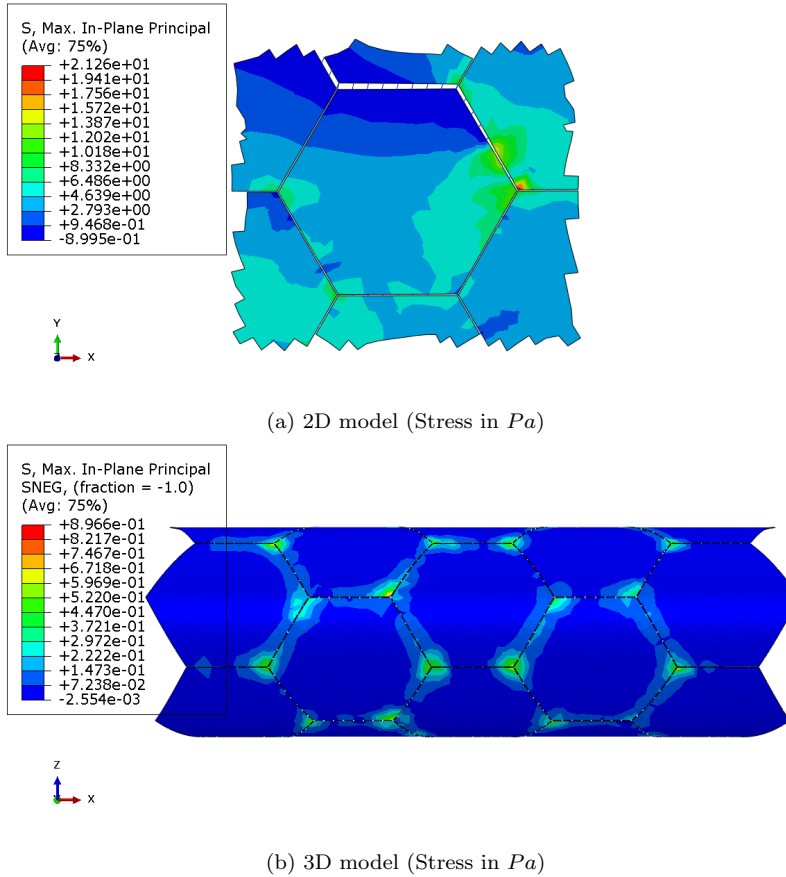


Figure 7: Stress concentration in the Endothelial Monolayer (Pa).

411 the deformation increases, which causes greater damage higher unbinding to
 412 the integrity of the endothelial barrier.

413 After the breaking phase, once the Calcium wave has passed, the cellu-
 414 lar contraction decreases and the joints are restored depending on whether
 415 they recover their original geometry. In the binding process, a “zip” effect is
 416 created where broken adhesions begin to bind mostly once the cellular con-
 417 traction ceases. This behavior is not the behavior that usually occurs in a
 418 monolayer, but it would be an extreme case of rupture. A more realistic scen-
 419 ario would be when the monolayer withstands stochastic damage resulting
 420 in the generation of specific gaps in certain areas between the cells.

421 In figure 11 we can observe the behavior of a single VE-cadherin connec-
 422 tion. At the beginning, in the absence of contraction, the force supported by

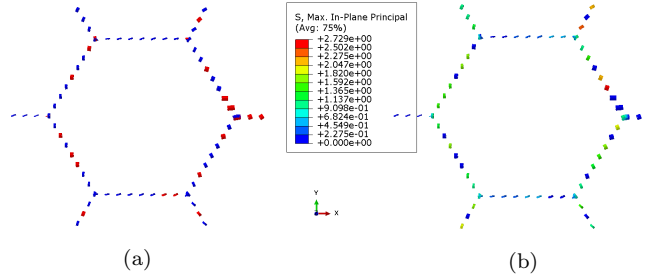


Figure 8: Unstable cell-cell adhesions in the endothelial monolayer. Only the joints are represented, as the cell in this case does not provide any information: (a) state of the adhesion: bound in blue and unbound in red; (b) Maximum principal stress in cell-cell adhesions (Pa). The appearance of the elements has been modified to improve visibility.

423 the adhesion is almost zero and it unbinds because of the instability charac-
 424 teristic of this phase (left part of figure 1). When the contraction begins to
 425 increase and the tensile forces increase, a rupture is observed (in $F = 6pN$).
 426 As there are no very high deformation, the adhesion is restored at around
 427 0.45 seconds and can resist forces higher than $10pN$ before the contraction
 428 disappears. When it is nearly free of forces in the final phase, it returns to
 429 the initial phase of instability with two unbinding events at low forces.

430 Finally, to investigate the influence of the radius of the blood vessel in
 431 the appearance of gaps we define the average damage of the adhesion in a
 432 period of time (T) as:

$$\bar{d}_T = \frac{\sum_{j=1}^m \sum_{i=1}^n d_{ij}}{nm} \quad (13)$$

433 where n is the number of increments in the analysis and m the number of
 434 total adhesions in the model.

435 Average damage in the adhesions increases when the contraction of cells
 436 increases. For the smaller radius it increases from 0.49% for a contraction
 437 of 1% to 0.64% for a contraction of 3%. However, there are no significant
 438 changes when the radius of the blood vessel increases, for example, for a
 439 contraction of 2%, we found that average damage ranges from 0.57% to
 440 0.595% for all simulated blood vessel radius.

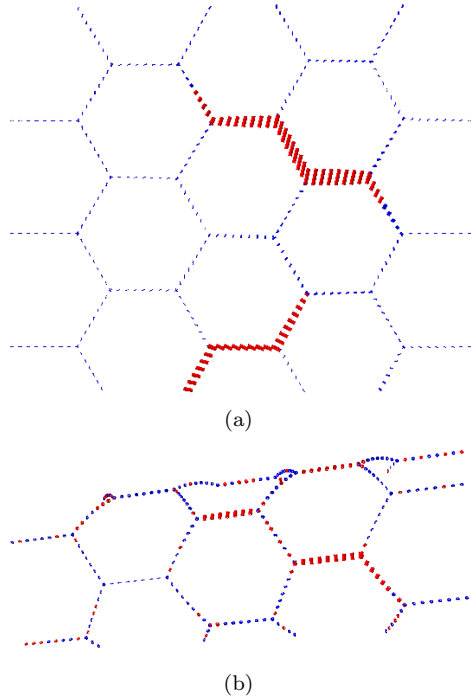


Figure 9: Pattern of rupture of the endothelial monolayer: (a) 2D model, blood vessel of radius infinity; (b) 3D model blood vessel of small radius. Blue means bound adhesion and red unbound adhesion.

441 4. Conclusions

442 In this work, we have proposed a hybrid model of three-dimensional en-
 443 dothelial monolayers. This model considers cells as linear elements of small
 444 thickness and adhesions as truss elements that can be bound and unbound
 445 depending on the mechanical environment by means of a catch-bond law.
 446 There are several models in literature, which study adhesion and gap forma-
 447 tion in blood vessels [2]. However, as far as we know, this is the first work,
 448 which simulates gap formation in three dimensions considering the blood
 449 vessel curvature. Even though we have observed no significant effect of the
 450 blood vessel diameter on the rupture of the adhesions of monolayer. The
 451 model shows how stress is more likely to accumulate in the vertices between
 452 three cells targeting this areas as location where extravasation is more likely
 453 to occur. This fact is in agreement with observation in other previous works
 454 [11, 2] where they observed in *in-vitro* experiments that gaps are more likely

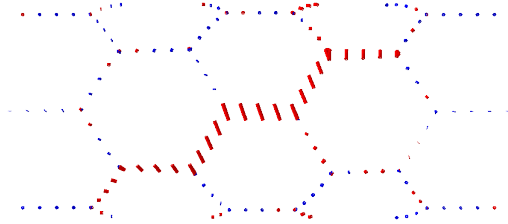


Figure 10: A crack generated in an endothelial monolayer with a radius of $8.32\mu m$ when there is a cellular contraction caused by a Calcium wave. Blue means bound adhesion and red unbound adhesion.

455 to occur in these vertices than in a two cell border.

456 To develop these simulations, several simplifications were necessary. First,
 457 we assume that the blood vessel diameter is constant during the simulation,
 458 so it does not change in response to cell contraction. Thus, we assume en-
 459 dothelial cells are perfectly joined to the vessel wall in the radial direction,
 460 and the vessel wall is rigid. A more realistic approach should include the prop-
 461 erties of the vessel and the characteristics of the adhesion of endothelial cells
 462 to the cell vessels, however deformation of cells in the radial direction will be
 463 smaller than the circumferential or longitudinal one. Second, adhesions could
 464 be activated when bound or deactivated when unbound; nevertheless, no new
 465 adhesions could be created when they were not present at the beginning of
 466 the simulation, even if cells change their position. Third, the geometry of the
 467 cell is assumed to be a regular hexagon in all the simulations; nevertheless,
 468 endothelial cells adapt their shape to the local requirements. In fact, previous
 469 works [43] observed that the endothelial cell monolayer is formed by regu-
 470 lar or non-regular hexagonal shape cells depending on the vessel curvature.
 471 However, we have not included this effect in the simulation.

472 The regulation of the endothelial monolayer plays a crucial role not only
 473 in the metastatic cascade but also in other pathologies such as pulmonary
 474 edema [54] and atherosclerosis [55]. It is also important for the immune
 475 system as it regulates exchanges of leukocyte between the bloodstream and
 476 the surrounding tissues [56]. Thus, the model we present in this work will
 477 be useful to understand these pathological and physiological conditions that
 478 crucially depend on extravasation.

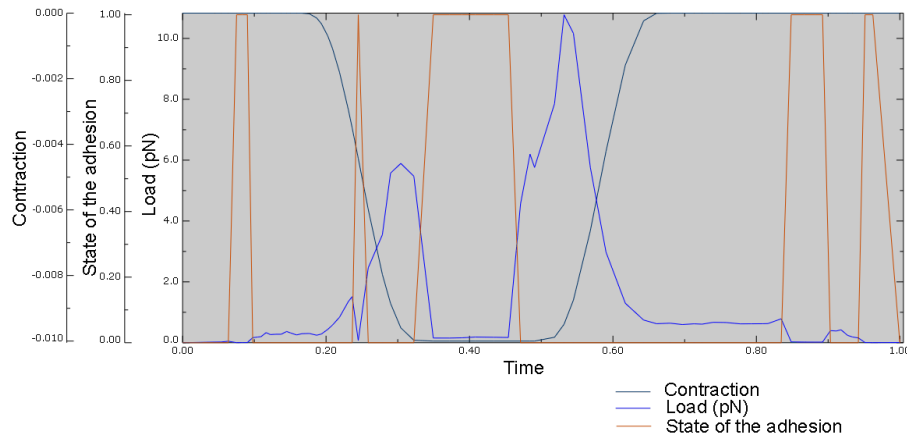


Figure 11: Diagram of evolution of load and state, bound (1) or unbound (0), of a cell-cell adhesion as a function of time (in seconds). The shown contraction is that the cells suffer when in contact with the adhesion.

479 5. Acknowledgements

480 Authors were supported by the European Commission (Grant no: 826494)
 481 and the Spanish Ministry of Economy and Competitiveness (Grant no: RTI2018-
 482 094494-B-C21).

483 References

- 484 [1] E. Dejana, F. Orsenigo, M. G. Lampugnani, The role of adherens junctions and VE-cadherin in the control of vascular permeability, *Journal of Cell Science* 121 (2008) 2115–2122. doi:10.1242/jcs.017897.
- 485
 486
- 487 [2] J. Escribano, M. B. Chen, E. Moeendarbary, X. Cao, V. Shenoy, J. M. Garcia-Aznar, R. D. Kamm, F. Spill, Balance of mechanical forces drives endothelial gap formation and may facilitate cancer and immune-cell extravasation, *Plos Computational Biology* 15(5) (2019) e1006395. doi:10.1371/journal.pcbi.1006395.
- 488
 489
 490
 491
- 492 [3] X. Cao, E. Moeendarbary, P. Isermann, P. M. Davidson, X. Wang, M. B. Chen, A. K. Burkart, J. Lammerding, R. D. Kamm, V. B. Shenoy, A chemomechanical model for nuclear morphology and stresses during cell transendothelial migration, *Biophysical Journal* 111 (2016) 1541 – 1552. doi:https://doi.org/10.1016/j.bpj.2016.08.011.
- 493
 494
 495
 496

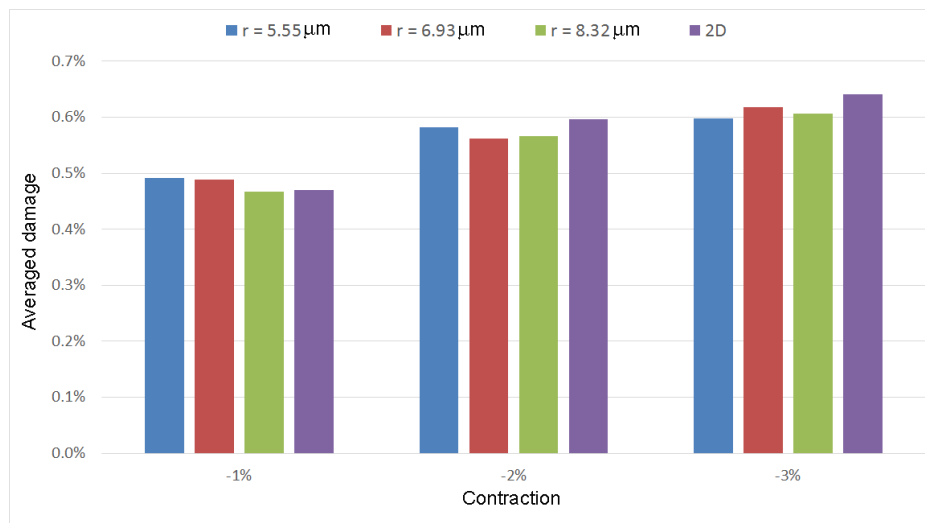


Figure 12: Averaged damage in the adhesion for the different blood vessels radius.

- 497 [4] J. Oldenburg, J. de Rooij, Mechanical control of the endothelial barrier,
 498 Cell and Tissue Research 355 (2014) 545–555. doi:10.1007/s00441-013-
 499 1792-6.
- 500 [5] R. Martinelli, A. S. Zeiger, M. Whitfield, T. E. Sciuto, A. Dvorak, K. J.
 501 Van Vliet, J. Greenwood, C. V. Carman, Probing the biomechanical
 502 contribution of the endothelium to lymphocyte migration: diapedesis
 503 by the path of least resistance, J Cell Sci 127 (2014) 3720–3734.
- 504 [6] S. Kumar, V. M. Weaver, Mechanics, malignancy, and metastasis: the
 505 force journey of a tumor cell., Cancer metastasis reviews 28 (2009)
 506 113–27. doi:10.1007/s10555-008-9173-4.
- 507 [7] H. Schnittler, Contraction of endothelial cells: 40 years of research,
 508 but the debate still lives, Histochemistry and Cell Biology 146 (2016)
 509 651–656. doi:10.1007/s00418-016-1501-0.
- 510 [8] M. A. Wozniak, C. S. Chen, Mechanotransduction in development: a
 511 growing role for contractility, Nature Reviews Molecular Cell Biology
 512 10 (2009) 34–43. doi:10.1038/nrm2592.
- 513 [9] B. Uygur, W.-S. Wu, SLUG promotes prostate cancer cell migration

- 514 and invasion via CXCR4/CXCL12 axis., *Molecular cancer* 10 (2011)
515 139. doi:10.1186/1476-4598-10-139.
- 516 [10] M. Mak, C. A. Reinhart-King, D. Erickson, Elucidating mechanical
517 transition effects of invading cancer cells with a subnucleus-scaled mi-
518 crofluidic serial dimensional modulation device., *Lab on a chip* 13 (2013)
519 340–8. doi:10.1039/c2lc41117b.
- 520 [11] J. S. Jeon, I. K. Zervantonakis, S. Chung, R. D. Kamm, J. L. Charest,
521 In vitro model of tumor cell extravasation, *PLOS ONE* 8 (2013) e56910.
522 doi:10.1371/journal.pone.0056910.
- 523 [12] K. Funamoto, D. Yoshino, K. Matsubara, I. K. Zervantonakis, K. Fu-
524 namoto, M. Nakayama, J. Masamune, Y. Kimura, R. D. Kamm, En-
525 dothelial monolayer permeability under controlled oxygen tension, *In-
526 tegrative Biology* 6 (2017) 529–538. doi:10.1039/c7ib00068e.
- 527 [13] E. T. Valent, G. P. van Nieuw Amerongen, V. W. M. van Hins-
528 bergh, P. L. Hordijk, Traction force dynamics predict gap forma-
529 tion in activated endothelium, *Experimental Cell Research* (2016).
530 doi:10.1016/j.yexcr.2016.07.029.
- 531 [14] J. Chen, D. Weihs, M. Van Dijk, F. J. Vermolen, A phenomenolog-
532 ical model for cell and nucleus deformation during cancer metastasis,
533 *Biomech Model Mechanobiol* 17 (2018) 1429–1450. doi:10.1007/s10237-
534 018-1036-5.
- 535 [15] I. Ramis-Conde, M. A. J. Chaplain, A. R. A. Anderson, D. Drasdo,
536 Multi-scale modelling of cancer cell intravasation: the role of cadherins
537 in metastasis, *Physical Biology* 6 (2009) 016008. doi:10.1088/1478-
538 3975/6/1/016008.
- 539 [16] I. González-Valverde, J. M. García-Aznar, A hybrid computational
540 model to explore the topological characteristics of epithelial tissues, *In-
541 ternational Journal for Numerical Methods in Biomedical Engineering*
542 (2017) e2877. doi:10.1002/cnm.2877.
- 543 [17] E. Y. M. Wong, L. Morgan, C. Smales, P. Lang, S. E. Gubby, J. M.
544 Staddon, Vascular endothelial growth factor stimulates dephosphoryla-
545 tion of the catenins p120 and p100 in endothelial cells, *Biochem. J* 346
546 (2000) 209–216.

- 547 [18] W. M. Briehar, A. S. Yap, Cadherin junctions and their cy-
548 toskelton(s), *Current Opinion in Cell Biology* 25 (2013) 39–46.
549 doi:10.1016/j.ceb.2012.10.010.
- 550 [19] A. M. Shewan, M. Maddugoda, A. Kraemer, S. J. Stehbins, S. Verma,
551 E. M. Kovacs, A. S. Yap, Myosin 2 is a key Rho kinase target necessary
552 for the local concentration of E-cadherin at cell-cell contacts., *Molecular*
553 *biology of the cell* 16 (2005) 4531–42. doi:10.1091/mbc.E05-04-0330.
- 554 [20] K. Ando, S. Fukuhara, T. Moriya, Y. Obara, N. Nakahata,
555 N. Mochizuki, Rap1 potentiates endothelial cell junctions by spatially
556 controlling myosin II activity and actin organization, *The Journal of*
557 *Cell Biology* 202 (2013) 901–916. doi:10.1083/jcb.201301115.
- 558 [21] M. G. Lampugnani, M. Corada, L. Caveda, F. Breviario, O. Ayalon,
559 B. Geiger, E. Dejana, The molecular organization of endothelial cell to
560 cell junctions: differential association of plakoglobin, beta-catenin, and
561 alpha-catenin with vascular endothelial cadherin (VE-cadherin)., *The*
562 *Journal of cell biology* 129 (1995) 203–17.
- 563 [22] A. Taddei, C. Giampietro, A. Conti, F. Orsenigo, F. Breviario, V. Pi-
564 razzoli, M. Potente, C. Daly, S. Dimmeler, E. Dejana, Endothelial
565 adherens junctions control tight junctions by VE-cadherin-mediated
566 upregulation of claudin-5, *Nature Cell Biology* 10 (2008) 923–934.
567 doi:10.1038/ncb1752.
- 568 [23] H. Lum, A. B. Malik, Mechanisms of increased endothelial permeability.,
569 *Canadian journal of physiology and pharmacology* 74 (1996) 787–800.
- 570 [24] D. E. Ingber, Mechanical signaling and the cellular response to extracel-
571 lular matrix in angiogenesis and cardiovascular physiology., *Circulation*
572 *research* 91 (2002) 877–87.
- 573 [25] P. E, O. HG, A model for individual and collective cell movement
574 in dictyostelium discoideum., *Proc Natl Acad Sci U S A.* (2000).
575 doi:10.1073/pnas.97.19.10448.
- 576 [26] N. J. Armstrong, K. J. Painter, J. A. Sherratt, A continuum approach to
577 modelling cell-cell adhesion, *Journal of Theoretical Biology* 243 (2006)
578 98 – 113. doi:10.1016/j.jtbi.2006.05.030.

- 579 [27] S. EV, V. V, T. WE, Catch-bond mechanism of force-enhanced adhesion:
580 counterintuitive, elusive, but ... widespread?, *Cell Host Microbe* (2008).
581 doi:10.1016/j.chom.2008.09.005.
- 582 [28] P. Panorchan, J. George, D. Wirtz, Probing intercellular interactions
583 between vascular endothelial cadherin pairs at single-molecule resolution
584 and in living cells., *Journal of Molecular Biology* (2006).
- 585 [29] K. Manibog, H. Li, S. Rakshit, S. Sivasankar, Resolving the molecular
586 mechanism of cadherin catch bond formation., *Nature Communications*
587 (2014).
- 588 [30] C. Buckley, J. Tan, K. Anderson, D. Hanein, N. Volkman, W. Weis,
589 W. Nelson, A. Dunn, The minimal cadherin-catenin complex binds to
590 actin filaments under force., *Science* (2014).
- 591 [31] E. A. Novikova, C. Storm, Contractile fibers and catch-bond clusters:
592 A biological force sensor?, *Biophysical Journal* 105 (2013) 1336–1345.
593 doi:10.1016/j.bpj.2013.07.039.
- 594 [32] D. Zeng, T. Juzkiw, A. T. Read, D. W.-H. Chan, M. R. Glucksberg,
595 C. R. Ethier, M. Johnson, Young’s modulus of elasticity of Schlemm’s
596 canal endothelial cells., *Biomechanics and modeling in mechanobiology*
597 9 (2010) 19–33. doi:10.1007/s10237-009-0156-3.
- 598 [33] N. Guz, M. Dokukin, V. Kalaparthi, I. Sokolov, If Cell Mechanics Can
599 Be Described by Elastic Modulus: Study of Different Models and Probes
600 Used in Indentation Experiments, *Biophysical Journal* 107 (2014) 564–
601 575. doi:10.1016/j.bpj.2014.06.033.
- 602 [34] J. Alcaraz, L. Buscemi, M. Grabulosa, X. Trepas, B. Fabry, R. Farré,
603 D. Navajas, Microrheology of Human Lung Epithelial Cells Measured
604 by Atomic Force Microscopy, *Biophysical Journal* 84 (2003) 2071–2079.
605 doi:10.1016/S0006-3495(03)75014-0.
- 606 [35] C. Tiruppathi, R. D. Minshall, B. C. Paria, S. M. Vogel, A. B. Malik,
607 Role of Ca²⁺ signaling in the regulation of endothelial permeability,
608 volume 39, 2002, pp. 173–185. doi:10.1016/S1537-1891(03)00007-7.
- 609 [36] M. Junkin, Y. Lu, J. Long, P. A. Deymier, J. B. Hoying, P. K.
610 Wong, Mechanically induced intercellular calcium communication in

- 611 confined endothelial structures, *Biomaterials* 34 (2013) 2049–2056.
612 doi:<https://doi.org/10.1016/j.biomaterials.2012.11.060>.
- 613 [37] J. Sun, J. B. Hoying, P. A. Deymier, D. D. Zhang, P. K. Wong, Cel-
614 lular architecture regulates collective calcium signaling and cell con-
615 tractility, *PLoS computational biology* 12 (2016) e1004955–e1004955.
616 doi:[10.1371/journal.pcbi.1004955](https://doi.org/10.1371/journal.pcbi.1004955).
- 617 [38] K. Garikipati, E. Arruda, K. Grosh, H. Narayanan, S. Calve, A con-
618 tinuum treatment of growth in biological tissue: the coupling of mass
619 transport and mechanics, *Journal of the Mechanics and Physics of Solids*
620 52 (2004) 1595 – 1625. doi:[10.1016/j.jmps.2004.01.004](https://doi.org/10.1016/j.jmps.2004.01.004).
- 621 [39] E. Reina-Romo, M. J. Gomez-Benito, J. M. Garcia-Aznar,
622 J. Dominguez, M. Doblare, Growth mixture model of distrac-
623 tion osteogenesis: effect of pre-traction stresses, *Biomech Model*
624 *Mechanobiol* 9 (2010) 103–115.
- 625 [40] L. Vujosevic, V. A. Lubarda, Finite-strain thermoelasticity based on
626 multiplicative decomposition of deformation gradient, *Theoretical and*
627 *Applied Mechanics* 28 (2002) 379–399. doi:[10.2298/TAM0229379V](https://doi.org/10.2298/TAM0229379V).
- 628 [41] T. Schmedt, Y. Chen, T. Nguyen, S. Li, J. Bonanno, U. V. Ju-
629 rkunas, Telomerase immortalization of human corneal endothelial
630 cells yields functional hexagonal monolayers, *PLoS ONE* (2012).
631 doi:[10.1371/journal.pone.0051427](https://doi.org/10.1371/journal.pone.0051427).
- 632 [42] R. D. O’Dea, J. R. King, Continuum limits of pattern formation in
633 hexagonal-cell monolayers., *Journal of Mathematical Biology* 64(3)
634 (2012) 579–610.
- 635 [43] M. Ye, H. M. Sanchez, M. Hultz, Z. Yang, M. Bogorad, A. D. Wong,
636 P. C. Searson, Brain microvascular endothelial cells resist elongation
637 due to curvature and shear stress., *Scientific reports* 4 (2014) 4681.
638 doi:[doi:10.1038/srep04681](https://doi.org/10.1038/srep04681).
- 639 [44] A. Pries, T. Secomb, P. Gaehtgens, The endothelial surface layer,
640 *Pflügers Archiv - European Journal of Physiology* 440 (2000) 653–666.
641 doi:[10.1007/s004240000307](https://doi.org/10.1007/s004240000307).

- 642 [45] F. M., The Endothelium, Morgan & Claypool Life Sciences, San Rafael
643 (CA), 2011.
- 644 [46] K. M. Stroka, H. Aranda-Espinoza, Endothelial cell substrate stiff-
645 ness influences neutrophil transmigration via myosin light chain kinase-
646 dependent cell contraction, *Blood* 118 (2011) 1632. doi:10.1182/blood-
647 2010-11-321125.
- 648 [47] P. F. Davies, A. Robotewskyj, M. L. Griem, Endothelial cell adhesion
649 in real time, *J. Clin. Invest.* 91 (1993) 2640–2652.
- 650 [48] M. Dehghan, N. Narimani, An element-free galerkin meshless method
651 for simulating the behavior of cancer cell invasion of surround-
652 ing tissue, *Applied Mathematical Modelling* 59 (2018) 500 – 513.
653 doi:10.1016/j.apm.2018.01.034.
- 654 [49] V. Mohammadi, M. Dehghan, Simulation of the phase field cahn-hilliard
655 and tumor growth models via a numerical scheme: Element-free galerkin
656 method, *Computer Methods in Applied Mechanics and Engineering* 345
657 (2019) 919 – 950. doi:10.1016/j.cma.2018.11.019.
- 658 [50] P. Wiedeman Mary, Dimensions of blood vessels from distributing
659 artery to collecting vein, *Circulation Research* 12 (1963) 375–378.
660 doi:10.1161/01.RES.12.4.375.
- 661 [51] W. C. Aird, Spatial and temporal dynamics of the en-
662 dothelium, *Journal of Thrombosis and Haemostasis* 3
663 (2005) 1392–1406. doi:10.1111/j.1538-7836.2005.01328.x.
664 arXiv:<https://onlinelibrary.wiley.com/doi/pdf/10.1111/j.1538-7836.2005.01328.x>
- 665 [52] M. A. Traore, S. C. George, Tissue engineering the vascular
666 tree, *Tissue engineering. Part B, Reviews* 23 (2017) 505–514.
667 doi:10.1089/ten.teb.2017.0010.
- 668 [53] K. Kruse, Y. A. Komarova, Tension across adherens junctions: when
669 less is more, *Oncotarget* 6(31) (2015) 30433–30434.
- 670 [54] S. R. Collins, R. S. Blank, L. S. Deatherage, R. O. Dull, Special arti-
671 cle: the endothelial glycocalyx: emerging concepts in pulmonary edema
672 and acute lung injury, *Anesthesia and analgesia* 117 (2013) 664–674.
673 doi:10.1213/ANE.0b013e3182975b85.

- 674 [55] S. Dimmeler, A. M. Zeiher, Vascular repair by circulating endothelial
675 progenitor cells: the missing link in atherosclerosis?, *Journal of Molec-*
676 *ular Medicine* 82 (2004) 671–677. doi:10.1007/s00109-004-0580-x.
- 677 [56] C. Strell, F. Entschladen, Extravasation of leukocytes in compari-
678 son to tumor cells, *Cell Communication and Signaling* 6 (2008) 10.
679 doi:10.1186/1478-811x-6-10.